THE JOURNAL OF BIOLOGICAL CHEMISTRY VOL. 289, NO. 48, pp. 33391–33403, November 28, 2014
Published in the U.S.A.

Asbestos-induced Disruption of Calcium Homeostasis Induces Endoplasmic Reticulum Stress in Macrophages*

Received for publication, May 7, 2014, and in revised form, October 10, 2014 Published, JBC Papers in Press, October 16, 2014, DOI 10.1074/jbc.M114.579870

Alan J. Ryan[‡], Jennifer L. Larson-Casey[§], Chao He[§], Shuhba Murthy[‡], and A. Brent Carter[‡§¶‖1]

From the Departments of [‡]Internal Medicine, [§]Radiation Oncology and Program in Free Radical and Radiation Biology, Carver College of Medicine, [¶]Human Toxicology, College of Public Health, University of Iowa, and [‖]Iowa City Veterans Administration Center, Iowa City, Iowa 52242

Background: Macrophages are important cells in fibrotic diseases.
Results: Chrysotile increases cytosolic calcium (Ca^{2+}) and induces endoplasmic reticulum (ER) stress in macrophages in a Ca^{2+}-dependent manner. ER stress is found in alveolar macrophages from fibrotic lungs.
Conclusion: Chrysotile triggers ER Ca^{2+} leak and induces ER stress in macrophages.
Significance: Macrophages undergo ER stress, which may contribute to pulmonary fibrosis.

Although the mechanisms for fibrosis development remain largely unknown, recent evidence indicates that endoplasmic reticulum (ER) stress and activation of the unfolded protein response (UPR) may act as an important fibrotic stimulus in diseased lungs. ER stress is observed in lungs of patients with idiopathic pulmonary fibrosis. In this study we evaluated if ER stress and the UPR was present in macrophages exposed to chrysotile asbestos and if ER stress in macrophages was associated with asbestos-induced pulmonary fibrosis. Macrophages exposed to chrysotile had elevated transcript levels of several ER stress genes. Macrophages loaded with the Ca^{2+}-sensitive dye Fura2-AM showed that cytosolic Ca^{2+} increased significantly within minutes after chrysotile exposure and remained elevated for a prolonged time. Chrysotile-induced increases in cytosolic Ca^{2+} were partially inhibited by either anisomycin, an inhibitor of passive Ca^{2+} leak from the ER, or 1,2-bis(2-aminophenoxyl)-ethane-*N*,*N*,*N*′,*N*′-tetraacetic acid (BAPTA-AM), an intracellular Ca^{2+} chelator known to deplete ER Ca^{2+} stores. Anisomycin inhibited X-box-binding protein 1 (XBP1) mRNA splicing and reduced immunoglobulin-binding protein (BiP) levels, whereas BAPTA-AM increased XBP1 splicing and BiP expression, suggesting that ER calcium depletion may be one factor contributing to ER stress in cells exposed to chrysotile. To evaluate ER stress *in vivo*, asbestos-exposed mice showed fibrosis development, and alveolar macrophages from fibrotic mice showed increased expression of BiP. Bronchoalveolar macrophages from asbestosis patients showed increased expression of several ER stress genes compared with normal subjects. These findings suggest that alveolar macrophages undergo ER stress, which is associated with fibrosis development.

Aberrant repair of injured tissue is a characteristic feature of fibrotic remodeling, including pulmonary fibrosis. A prototypical type of pulmonary fibrosis is caused by asbestos exposure, which is prevalent worldwide as at least 125 million are exposed to hazardous levels, including 1.3 million workers in the United States (1). The pathogenesis of asbestosis is not fully understood; however, recent evidence suggests that endoplasmic reticulum (ER)[2] stress and activation of the unfolded protein response (UPR) may contribute to fibrosis development in a variety of tissues, including the lung (2, 3).

The ER is involved in many cellular functions, including calcium (Ca^{2+}) storage and signaling and the folding and maturation of proteins. Conditions such as ER Ca^{2+} depletion, oxidative stress, viral infections, glucose deprivation, and environmental exposures can impair ER function leading to accumulation of unfolded or misfolded proteins in the ER lumen (4, 5). Cells respond to ER stress by activating a homeostatic signaling network, the UPR. The UPR is designed to attenuate ER stress and consists of three adaptive signaling pathways that act to restore ER protein folding capacity via: 1) decreasing protein load by inhibiting translation; 2) increasing ER chaperone proteins by transcriptional up-regulation; and 3) increasing ER-associated protein degradation of unfolded proteins. The UPR includes three ER resident transmembrane proteins, inositol-requiring enzyme 1 (IRE-1), PKR-like ER kinase, and activating transcription factor 6 (ATF6) that act as sensors by monitoring ER protein folding status. Under basal conditions, these proteins are bound by the ER chaperone BiP (immunoglobulin-binding protein or glucose-regulated protein 78-kDa, GRP78) and are maintained in an inactive state. When ER stress develops and unfolded proteins accumulate, BiP is released from IRE-1, PKR-like ER kinase, and ATF6, which triggers activation of the downstream pathways of the UPR. Although the UPR is designed to alleviate ER stress, prolonged or severe UPR activation

* This work was supported, in whole or in part, by National Institutes of Health Grants 2 ROI ES 015981-08 and P30 CA086862 and by Merit Review from the Department of Veteran Affairs, Office of Research and Development, Biomedical Laboratory Research and Development Grant 1 BX001135-01.
[1] To whom correspondence should be addressed: C33 GH, University of Iowa Carver College of Medicine, Iowa City, IA 52242. E-mail: brent-carter@uiowa.edu.

[2] The abbreviations used are: ER, endoplasmic reticulum; AEC, alveolar epithelial cells; ATF6, activating transcription factor 6; BAL, bronchoalveolar lavage; BiP, immunoglobulin binding protein; CHOP, DNA-damage inducible protein; ERO1-α, endoplasmic oxidase 1-α; GRP, glucose-regulated protein; FCCP, carbonyl cyanide *p*-trifluoromethoxyphenylhydrazone; IP_3R-1, inositol 1,4,5-triphosphate receptor; IRE-1, inositol-requiring enzyme 1; TiO_2, titanium dioxide; UPR, unfolded protein response; XBP-1, X-box binding protein 1; HBSS, Hanks' balanced salt solution; BMDM, bone marrow-derived macrophages; BAPTA-AM, 1,2-bis(2-aminophenoxyl)-ethane-*N*,*N*,*N*′,*N*′-tetraacetic acid.

can modulate inflammation and initiate programmed cell death contributing to the pathogenesis of various human diseases (4–6).

ER stress in alveolar type II cells (AEC) has been shown to be present in fibrotic loci in patients with pulmonary fibrosis (7, 8). ER stress in AECs can be induced by mutations in surfactant protein C (8, 9), mutations in SPA (10), and chronic herpesvirus infection (9, 11), and ER stress can result in intrinsic apoptosis secondary to mitochondrial dysfunction (12). UPR markers and increased collagen Type I expression have been observed in fibroblasts of fibrotic lungs, a response likely mediated by activation of TGF-β signaling (7). Alveolar macrophages have an important role in fibrosis development (13–15); however, the role of ER stress in macrophages in pulmonary fibrosis has not been investigated.

Depletion of ER Ca^{2+} stores can induce ER stress (16). Thapsigargin, a strong inducer of ER stress, selectively inhibits the ER Ca^{2+}-ATPase (17), which reduces active transport of Ca^{2+} into the ER lumen resulting in increases in cytosolic Ca^{2+} (18) as well as gradual depletion of ER Ca^{2+} stores. Because BiP and other chaperones are Ca^{2+}-binding proteins, ER Ca^{2+} depletion impairs chaperone activity resulting in accumulation of unfolded proteins and activation of an ER stress response. Recent studies using thapsigargin in combination with Ca^{2+} chelator BAPTA-AM to deplete ER Ca^{2+} stores have shown induction of the UPR in endothelial cells (19) and PC12 cells (20). Notably, ER Ca^{2+} leak through the translocon was recently revealed as a possible mechanism for ER Ca^{2+} depletion leading to activation of the UPR (21, 22).

Disruption of Ca^{2+} homeostasis has not been directly linked to fibrotic conditions, and the role of Ca^{2+} depletion and ER stress in macrophages in the development of pulmonary fibrosis is not known. The objective of this study was to determine whether chrysotile asbestos elicits ER stress secondary to alterations ER Ca^{2+} release in macrophages. To provide biological relevance, we determined if alveolar macrophages exhibit ER stress markers in chrysotile-exposed fibrotic mice and in patients with asbestosis.

EXPERIMENTAL PROCEDURES

Materials—Chrysotile asbestos was provided by Dr. Peter S. Thorne, University of Iowa College of Public Health. Chrysotile stock solutions (10 mg/ml) were prepared in PBS without calcium or magnesium, stored at −20 °C, and vortexed vigorously before use. Fura2-AM, Fluo-3-AM, and ionomycin were from Invitrogen. Rabbit BiP/GRP78 antibody was obtained from Cell Signaling, and mouse monoclonal ATF6 antibody and FCCP (carbonyl cyanide *p*-trifluoromethoxyphenylhydrazone) were from Abcam. Human inositol 1,4,5-triphosphate receptor (IP_3R-1) siRNA was from Santa Cruz Biotechnology, Inc. β-Actin antibody, thapsigargin, and tunicamycin were obtained from Sigma, and ansiomycin was from Millipore. The mouse transforming growth factor β1 (TGF-β1) Duo Set Elisa kit was obtained from R&D Systems, Inc.

Human Subjects—The Human Subjects Review Board of the University of Iowa Carver College of Medicine approved the protocol of obtaining alveolar macrophages from normal volunteers and patients with asbestosis. Normal volunteers had to meet the following criteria: 1) age between 18 and 55 years; 2) no history of cardiopulmonary disease or other chronic disease; 3) no prescription or nonprescription medication except oral contraceptives; 4) no recent or current evidence of infection; and 5) lifetime nonsmoker. Alveolar macrophages were also obtained from patients with asbestosis. Patients with asbestosis had to meet the following criteria: 1) FVC and DLCO at least 50% predicted; 2) current nonsmoker; 3) no recent or current evidence of infection; and 4) evidence of restrictive physiology on pulmonary function tests and interstitial fibrosis on chest computed tomography. Fiber optic bronchoscopy with bronchoalveolar lavage was performed after subjects received intramuscular atropine (0.6 mg) and local anesthesia. Three subsegments of the lung were lavaged with five 20-ml aliquots of normal saline, and the first aliquot in each was discarded. The percentage of alveolar macrophages was determined by Wright-Giemsa stain and varied from 90 to 98%.

Mice—C57BL/6 mice were purchased from Jackson Laboratories. All protocols were approved by the University of Iowa Institutional Animal Care and Use Committee. Mice were anesthetized with 3% isoflurane using a precision Fortec vaporizer (Cyprane, Keighley, UK) and then given either 125 μg of titanium dioxide (TiO_2) or 125 μg of chrysotile asbestos in 75 μl of 0.9% saline by the intratracheal route. Mice were euthanized 21 days after chrysotile exposure, a time interval that elicits histological and biochemical evidence of pulmonary fibrosis in mice (14). Bronchoalveolar lavage (BAL) was performed and BAL cells were isolated for differential cell counts and RNA isolation. Lungs were removed and fixed in formalin for assessment of collagen deposition using Masson's trichrome staining and by hydroxyproline assay.

Cell Culture—The human monocytic THP-1 cell line was obtained from American Type Culture Collection. Cells were maintained in RPMI 1640 medium containing 10 mM HEPES, 1 mM sodium pyruvate, 2.5 g/liter of glucose, 2 mM L-glutamine, 10% fetal bovine serum, and penicillin/streptomycin. For experiments, THP1 cells ($\sim 1 \times 10^6$ cells/ml) were incubated in RPMI medium, phenol red-free, containing 0.5% fetal bovine serum. Bone marrow-derived macrophages (BMDM) were isolated from C57BL/6 mice femur and tibia bones according protocols described by Weischenfeldt and Porse (23). Briefly, isolated BMDM were grown in culture dishes in DMEM containing 10% fetal bovine serum, penicillin/streptomycin, and supplemented with 10% L929 conditioned medium as a source of macrophage colony-stimulating factor. Cells were grown for 6–7 days and then plated in 6-well dishes at a density of $\sim 1.5 \times 10^6$ cells/well for an additional 24 h. Cells were cultured in phenol red-free RPMI medium containing 0.5% fetal bovine serum for experiments.

Immunoblot Analysis—Cell protein lysates were harvested in lysis buffer (50 mM Tris, pH 7.4, 150 mM NaCl, and 1% Nonidet P-40) containing a protease inhibitor mixture (Roche Applied Science, Complete Mini tablets) and a phosphatase inhibitor mixture (Calbiochem no. 524625). Cell lysates were sonicated for 30 s and cleared by centrifugation (10,000 × *g* at 4 °C). Supernatants were assayed for protein content using a DC™ Protein Assay kit (Bio-Rad). Lysates (10–50 μg) were separated by SDS-PAGE, transferred to PVDF membranes, and immunoblot analysis was conducted as described (24). Primary antibody

dilutions used for GRP78/BiP (1:1000), ATF6 (1:1000), and β-actin (1:40,000) were followed by the appropriate secondary antibody cross-linked to horseradish peroxidase. Protein bands were visualized by enhanced chemiluminescence (Amersham Biosciences ECL Prime) and quantified by densitometry using ImageJ software (NIH).

Real-time RT-PCR—Quantitative RT-PCR was conducted by isolating total RNA using TRIzol Reagent (Invitrogen) and synthesizing cDNA from 1–2 μg of RNA using the iScript™ cDNA Synthesis Kit (Bio-Rad). PCR was conducted using iQ™ SYBR® Green Supermix (Bio-Rad) with target cDNA and 15 pmol of reverse and forward gene-specific primers as follows: 3 min at 95 °C, then 45 cycles of 95 °C for 20 s, 60 °C for 20 s, and 72 °C for 20 s. Amplification specificity was confirmed by a melting curve analysis. Sample mRNA abundance was calculated using the cycle threshold ($\Delta\Delta C_T$) method. The relative expression of each gene was normalized to the quantity of hypoxanthine-guanine phosphoribosyltransferase or β-actin. Gene-specific primers were designed using the NCBI sequence database and were purchased from Integrated DNA Technologies (Coralville, IA).

XBP1 mRNA Splicing Assay—Splicing of X-box binding protein 1 (XBP1) mRNA is used as a measure of IRE-1 activation. Conventional RT-PCR was conducted to detect the presence of XBP1 mRNA splicing (25). Total RNA was isolated and cDNA was synthesized as described above. The following primers were used to amplify both unspliced and spliced human XBP1 mRNA: XBP1-F, 5′-TTA CGA GAG AAA ACT CAT GGC C-3′ and XBP1-R, 5′-GGG TCC AAG TTG TCC AGA ATG C-3′ to yield products of 289 and 263 bp, respectively. Primers used for unspliced and spliced mouse XBP1 mRNA: GAA CCA GGA GTT AAG AAC ACG and AGG CAA CAG TGT CAG AGT CC to yield products of 205 and 179 bp, respectively. PCR was conducted using target cDNA with Phusion DNA polymerase (New England Biolabs) as follows: 2 min at 98 °C, then 35 cycles of 98 °C for 20 s, 52 °C for 30 s, 72 °C for 20 s followed by 1 min at 72 °C. PCR products were separated in a 10% acrylamide gel and the bands were visualized by silver staining.

Measurement of Cytosolic Ca^{2+}—Human THP1 cells were loaded with Fura2-AM (1 μM, 30 min, 37 °C) at a cell density of 1×10^6 cells/ml in RPMI medium. Cells were washed twice in Hanks balanced salt solution (HBSS, Invitrogen) containing 1.3 mM $CaCl_2$ or Ca^{2+}-free HBSS. HBSS had the base composition of 138 mM NaCl, 1.0 mM $MgCl_2$, 5.3 mM KCl, 4.2 mM $NaHCO_3$, 0.45 mM KH_2PO_4, 0.33 mM Na_2HPO_4, pH 7.3, and 5.6 mM glucose. After washing, cells were suspended in Ca^{2+} containing or Ca^{2+}-free HBSS and incubated a further 30 min to allow for acetoxymethyl (AM) esterase cleavage. In some experiments, cells were loaded with BAPTA-AM (1–5 μM, 30 min, 37 °C) using the same procedures. Suspended cells were loaded into a 96-well plate (~1.75×10^5 cells/well) and placed into a SpectroMax M2 plate reader (Molecular Devices) set at 37 °C for fluorescence measurements. Fura2 dye was excited through 340- and 380-nm filters and fluorescence emission was collected at 510 nm. Data collection at 1–10-min intervals was performed using SoftMax Pro 6.1 software (Molecular Devices). The ratio of fluorescence intensity of 340/380 nm (F_{340}/F_{380}) was used to determine intracellular free calcium.

Confocal Microscopy—THP1 cells were loaded with Fluo-3 AM (2.5 μM, 60 min, 37 °C), washed twice in HBSS, suspended in RPMI medium 1640 containing 0.5% bovine serum, and placed in chambered coverslips. Fluorescence images were collected using a Zeiss 510 LSM Confocal Microscope. Fluo-3 dye was excited at 488 nm and emission collected by a 475–500-nm filter.

siRNA Transfection—siRNA against human IP3R-1 was from Santa Cruz Biotechnology, Inc. (sc-42475) and described as a pool of three target specific 19–25-nucleotide siRNA designed to knockdown human IP3R-1 gene expression. The IP3R-1 siRNA (100 nM) was transfected into THP1 cells (~0.5×10^6 cells/ml) using DharmaFECT 2 transfection reagent (Dharmacon Research, Inc.) according to manufacturer's instructions. After 6 h of transfection, the medium was switched to RPMI 1640 medium containing 10% FBS, and 48 h later, the indicated experiments were conducted.

Hydroxyproline Assay—Lung tissue was dried at 100 °C to a stable weight and hydrolyzed with 6 N HCl for 24 h at 112 °C. Lung hydroxyproline content was determined as described (14) and expressed relative to lung dry weight.

Statistical Analysis—A Student's unpaired, two-tailed *t* test was used to assess statistical differences between two groups. A one-way analysis of variance was used when comparing more than two groups with Tukey post hoc test to determine differences. Data were expressed as mean ± S.E. Probability values $p < 0.05$ were considered significant.

RESULTS

Chrysotile Induces ER Stress in Macrophages—To determine whether chrysotile induces an ER stress response in macrophages, we first examined the IRE/XBP1 pathway. Activation of the IRE1/XBP1 pathway results in the splicing of a 26-bp fragment from the mRNA encoding transcription factor XBP1. XBP1 mRNA splicing generates an active XBP1 transcription factor that acts as a potent inducer of select ER stress genes. Macrophages exposed to chrysotile showed splicing of XBP1 mRNA after 24 h, but not at earlier time intervals (Fig. 1*A*). In contrast, thapsigargin (100 nM), an ER Ca^{2+}-ATPase inhibitor used as a positive control, elicited significant XBP1 splicing within 3–6 h.

BiP is known as a master regulator of the ER stress response (6), thus we evaluated the expression of BiP as well as the ER stress transcriptional enhancer ATF6α by immunoblot analysis. Macrophages exposed to chrysotile for 24 and 48 h showed increased levels of BiP as well as elevated ATF6α (Fig. 1*B*). Densitometric quantification of immunoblots revealed an increase in normalized BiP protein in macrophages exposed for 24 h to chrysotile or thapsigargin (Fig. 1*C*). We assessed macrophage BiP mRNA expression by quantitative real-time RT-PCR after chrysotile exposure and found increased BiP mRNA levels at 24 and 48 h, but not at earlier times (3–6 h) after exposure (Fig. 1*D*). We also examined mRNA expression of other chaperone genes, and found that GRP94, endoplasmic-resident protein 72, and protein kinase inhibitor 58-kDa transcripts were increased after 24 h chrysotile exposure (Fig. 1, *E*–*G*). Notably these ER

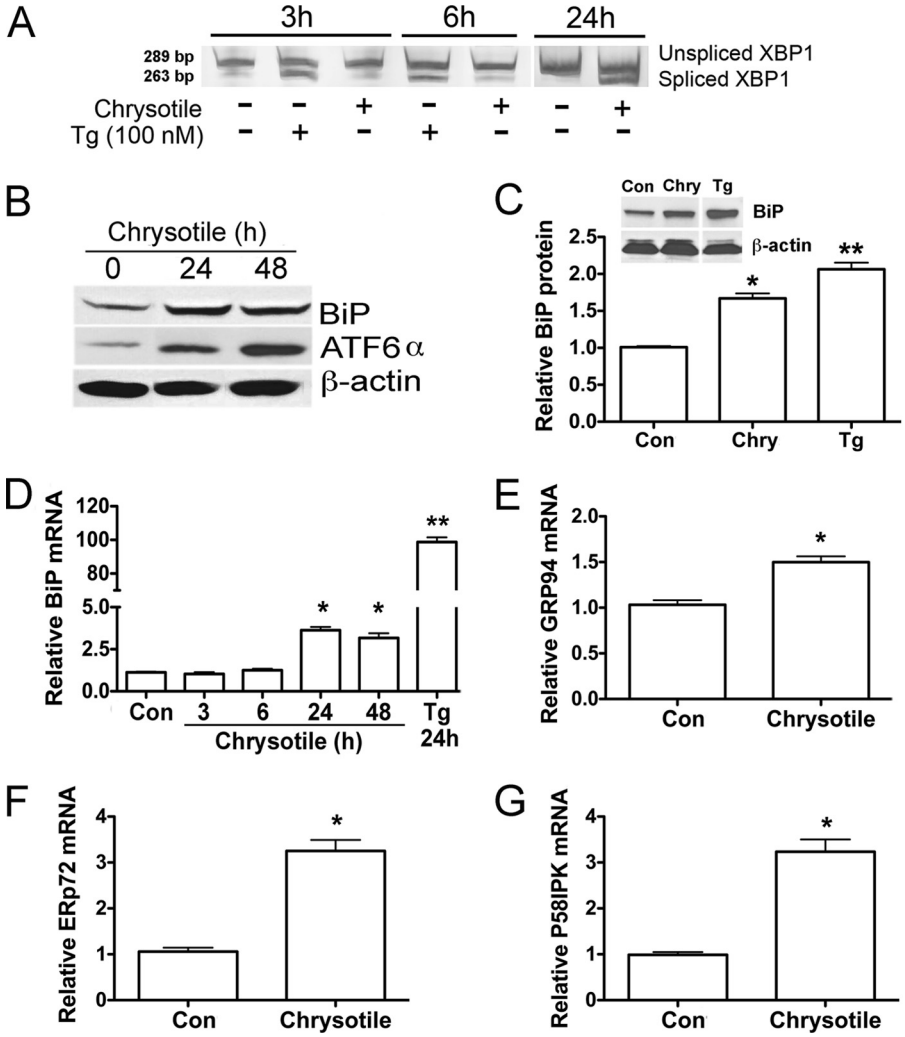

FIGURE 1. **Chrysotile induces ER stress in macrophages.** *A,* macrophages were exposed to thapsigargin (*Tg*, 100 nM) or chrysotile (10 μg/cm^2) for the indicated times. Spliced XBP1 was evaluated by conventional RT-PCR followed by acrylamide gel electrophoresis. *B,* macrophages exposed to chrysotile (10 μg/cm^2) for 24 or 48 h and cell lysates were used for GRP 78/BiP and ATF6 expression by protein immunoblot analysis. *C*, densitometric analysis of BiP protein expression corrected for β-actin in cells exposed to chrysotile (*Chry*) or thapsigargin for 24 h. * or **, $p < 0.05$ *versus* control or thapsigargin or Chry. $n = 8$/group. *Inset* shows an BiP immunoblot for a 24-h exposure. *D,* quantitative RT-PCR for BiP mRNA corrected for hypoxanthine-guanine phosphoribosyltransferase mRNA. Macrophages were treated with chrysotile for the indicated times or thapsigargin for 24 h. * or **, $p < 0.05$ *versus* other groups. $n = 8$/group. *E–G*, quantitative RT-PCR data showing mRNA of different ER stress genes corrected for hypoxanthine-guanine phosphoribosyltransferase mRNA. $n = 3$/group. RNA was isolated from macrophages 24 h after exposure to chrysotile (10 μg/cm^2). *, $p < 0.05$ *versus control*. $n = 3$/group.

stress genes are modulated, at least in part, by ATF6α (26, 27). Taken together, these results demonstrate activation of the ER stress response in macrophages exposed to chrysotile.

To determine whether chrysotile elicited ER stress in primary macrophage cells, mouse BMDM were isolated and treated with the ER Ca^{2+}-ATPase inhibitor, thapsigargin (100 nM), or with an inhibitor of *N*-linked glycosylation, tunicamycin (5 μg/ml). BMDM exposed to chrysotile, thapsigargin, or tunicamycin for 24 h showed splicing of XBP1 mRNA (Fig. 2*A*) as well as increased levels of BiP protein (Fig. 2, *B* and *C*), BiP mRNA (Fig. 2*D*), and DNA-damage inducible protein (CHOP) mRNA (Fig. 2*E*). Because current evidence suggests that ER stress can act as a pro-fibrotic stimulus (3) and because TGF-β1 can induce ER stress in lung fibroblasts (7), we asked if pro-fibrotic gene expression was detected in macrophages under ER stress. Interestingly, we found increased levels TGF-β1 mRNA in BMDM cells exposed to chrysotile or thapsigargin, whereas TGF-β1 transcript levels remained unchanged in cells exposed to tunicamycin for 24 h (Fig. 2*F*). These findings support the idea that chrysotile elicits ER stress in macrophages and, furthermore, that increased expression of pro-fibrotic TGF-β1 is associated with ER stress in these cells.

Chrysotile-induced Alterations in Calcium Flux Are Linked to the ER Stress Response—Because asbestos-induced Ca^{2+} release has been associated with ER stress in AECs (12) and because ER Ca^{2+} depletion has been linked to ER stress (16), we determined if Ca^{2+} release occurred in macrophages exposed to chrysotile. For our initial assessments, cells were loaded with Fluo3-AM and evaluated by confocal microscopy. Chrysotile exposure increased cytosolic Ca^{2+} (Fig. 3*A*). In subsequent experiments, cells were loaded with Fura2-AM and exposed to chrysotile to evaluate time-dependent changes in Ca^{2+} release. Cytosolic Ca^{2+} levels were significantly increased above controls and remained elevated for the duration of the experiment (Fig. 3*B*). Addition of ionomycin, a Ca^{2+} ionophore, stimulated further increases in cytosolic Ca^{2+} levels (Fig. 3*B*), whereas addition of

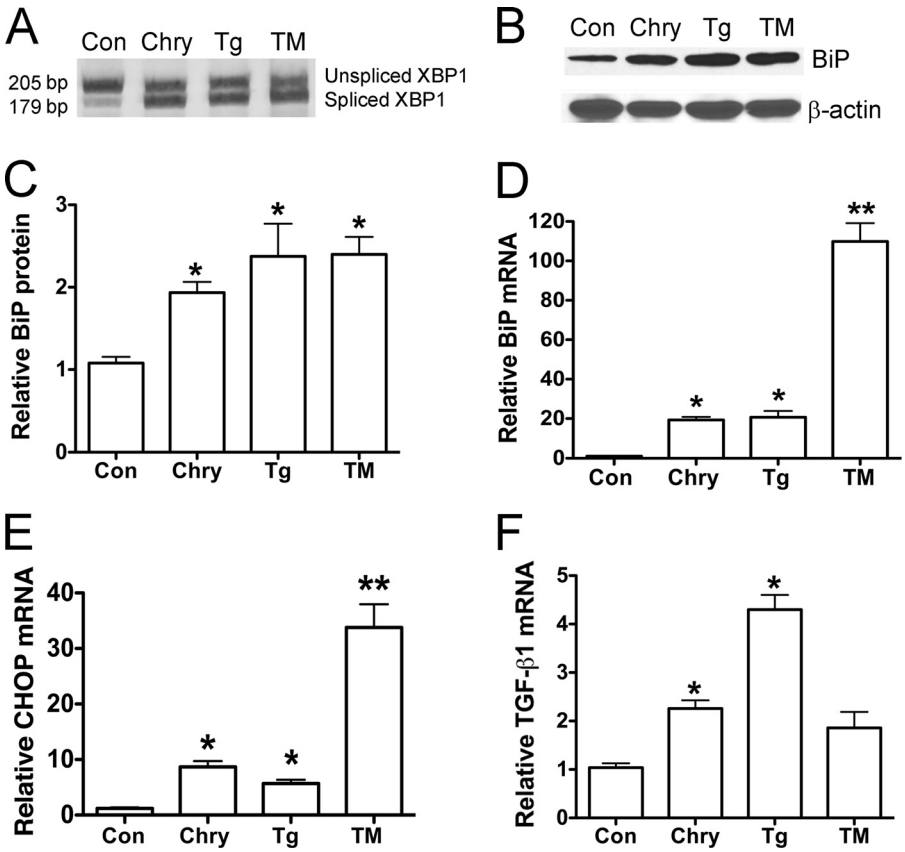

FIGURE 2. **Chrysotile induces ER stress in bone marrow-derived macrophages.** *A,* macrophages were exposed to chrysotile (10 μg/cm^2), thapsigargin (*Tg*, 100 nM), or tunicamycin (*TM*, 5 μg/ml) for 24 h, and then assayed for XBP1 splicing using conventional RT-PCR plus acrylamide gel electrophoresis. Data from experiments conducted as described in *A* are shown: *B,* immunoblot analysis for BiP protein and β-actin; *C,* densitometric analysis of BiP protein expression was corrected for β-actin (*, $p < 0.05$ *versus* control). *D–F*, quantitative RT-PCR data showing relative BiP mRNA, relative CHOP mRNA, and relative TGFβ1 mRNA corrected β-actin. *, $p < 0.05$ *versus* control; **, $p < 0.05$ *versus* other groups. $n = 6$–10/group.

EDTA, a Ca^{2+} chelator, dramatically reduced cytosolic Ca^{2+} (Fig. 3*C*). When cells were exposed to chrysotile in Ca^{2+}-free medium, cytosolic Ca^{2+} increased, implicating the ER as an important source for Ca^{2+} in these cells (Fig. 3*D*). When $CaCl_2$ was added, further increases in cytosolic Ca^{2+} were observed (Fig. 3*D*).

Because ER Ca^{2+} depletion and ER stress have been induced in cells loaded with the intracellular Ca^{2+} chelator, BAPTA-AM (20), we examined the effects of BAPTA-AM in macrophages exposed to chrysotile. Chrysotile steadily increased cytosolic Ca^{2+} levels in a time-dependent manner to values 5–6-fold above control values (Fig. 3*E*). However, BAPTA-AM reduced cytosolic Ca^{2+} levels below control values, and also inhibited the chrysotile-induced increases in cytosolic Ca^{2+} throughout the 180-min chrysotile exposure. During the final minutes of incubation, we added the mitochondrial uncoupler FCCP and observed sharp increases in cytosolic Ca^{2+}, a response indicating cells were viable and actively regulating cellular Ca^{2+} before FCCP exposure (Fig. 3*E*). To determine whether BAPTA-AM induces ER stress in macrophages, we loaded cells with BAPTA-AM and incubated the cells for 24 h. BAPTA-AM elicited XBP1 splicing (Fig. 3*F*) and increased BiP protein (Fig. 3*G*) and BiP mRNA levels (Fig. 3*H*). Collectively, these findings demonstrate that chrysotile elicits sustained increases in cytosolic Ca^{2+} levels, and suggests that depletion of intracellular Ca^{2+} stores is linked to ER stress in macrophages.

Recent evidence indicates that ER calcium depletion during ER stress may occur by Ca^{2+} leak through the translocon, an ER protein complex involved in translation (21, 22). Furthermore, an inhibitor of translocon Ca^{2+} leak, anisomycin, has been shown to alter the ER stress response in certain cell types (28). To assess if anisomycin modulates Ca^{2+} flux in macrophages, Fura2-AM-loaded cells were pretreated with anisomycin before chrysotile exposure. As anticipated, anisomycin inhibited the chrysotile-induced increases in cytosolic Ca^{2+} in macrophages suspended in 1.3 mM Ca^{2+} medium (Fig. 4*A*) and in Ca^{2+}-free medium (Fig. 4*B*). Anisomycin also inhibited BiP protein expression (Fig. 4, *C* and *D*), BiP mRNA levels (Fig. 4*E*), as well as XBP1 mRNA splicing (Fig. 4*F*). In aggregate, these data suggest that inhibition of the translocon reduces chrysotile-induced ER Ca^{2+} release and attenuates the ER stress response.

To further evaluate how chrysotile-induced ER Ca^{2+} release is related to the ER stress response in macrophages, we conducted comparative experiments examining cytosolic Ca^{2+} levels in cells exposed to chrysotile or cells exposed to ER stress inducing agents thapsigargin and tunicamycin. We first examined cytosolic Ca^{2+} levels in cells acutely exposed to chrysotile, thapsigargin, or tunicamycin and found that chrysotile elicited prolonged increases in cytosolic Ca^{2+} compared with transient elevations in cytosolic

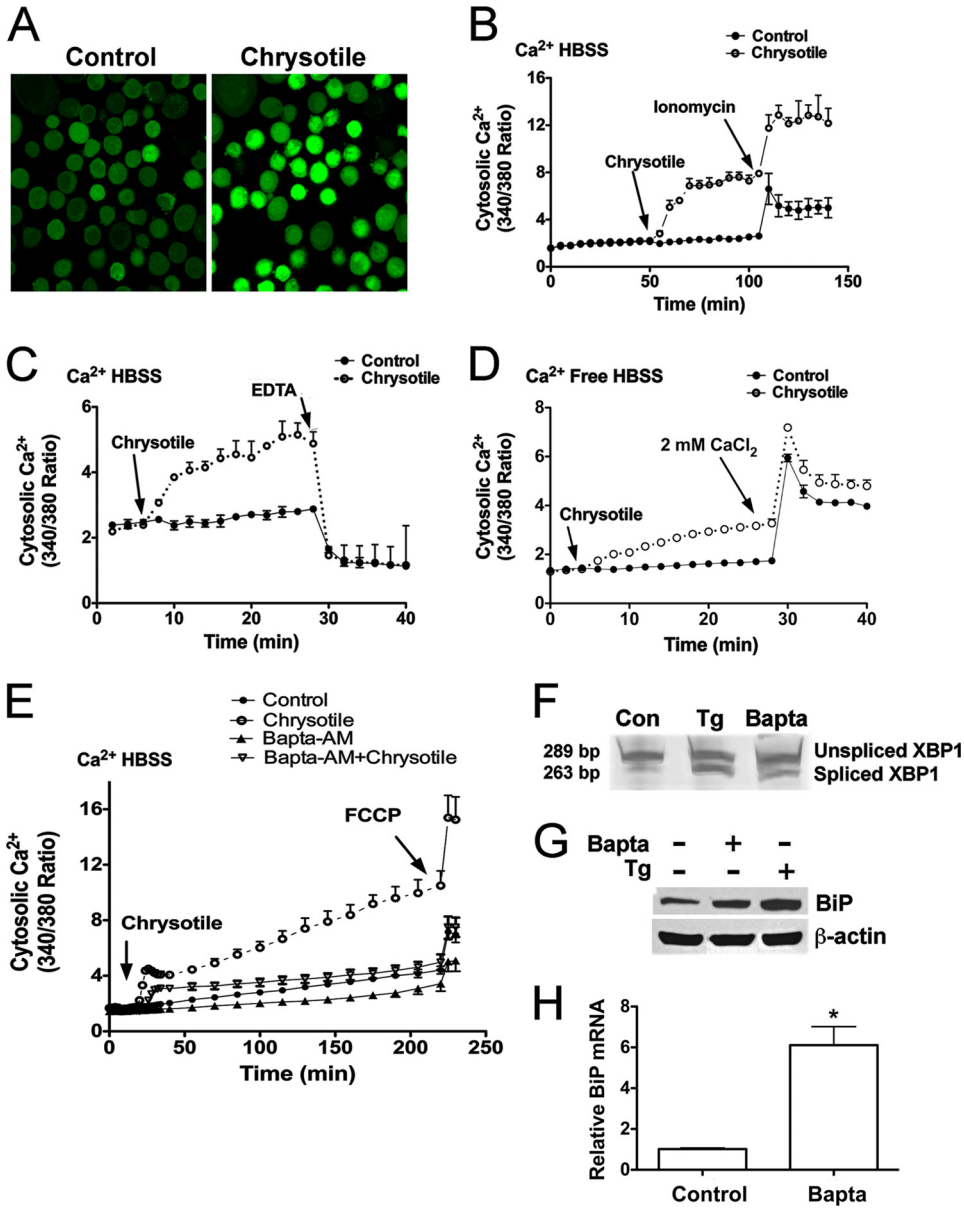

FIGURE 3. **Chrysotile increases cytosolic Ca^{2+} levels in macrophages.** *A*, cells were loaded with Fluo3-AM (2.5 μM, 1 h, 37 °C) and then exposed to chrysotile (10 $\mu g/cm^2$) for evaluation by confocal microscopy. Cells were loaded with Fura2-AM (1 μM, 30 min, 37 °C), suspended in HBSS containing 1.3 mM Ca^{2+}, and exposed to chrysotile (10 μg/well) followed by (*B*) 5 μM ionomycin or (*C*) 2 mM EDTA. Values are mean ± S.E. ($n = 3$/group). *D*, cells were loaded with Fura2-AM as above stated, suspended in Ca^{2+}-free HBSS, exposed to chrysotile (10 $\mu g/cm^2$) followed by 2 mM $CaCl_2$. *E*, cells were loaded with Fura2-AM (1 μM, 30 min, 37 °C) and Ca^{2+} chelator BAPTA-AM (1 μM, 30 min, 37 °C) 30 min before chrysotile exposure. The proton ionophore FCCP (5 μM) was used as a positive control. $n = 6$/group. Cells were exposed to BAPTA-AM (5 μM, 24 h) and assayed for (*F*) spliced XBP1, by conventional RT-PCR plus gel electrophoresis as well as (*G*) BiP protein expression by immunoblot analysis, and (*H*) BiP mRNA expression by quantitative RT-PCR. Thapsigargin (*Tg*) (100 nM) for 24 h was used as a positive control. *, $p < 0.05$ *versus* control ($n = 6$/group).

Ca^{2+} following thapsigargin or tunicamycin treatments (Fig. 5, *A* and *B*). Notably, after 150 min of exposure, the addition of 2 mM $CaCl_2$ triggered rapid and relatively large increases in cytosolic Ca^{2+} in cells treated with thapsigargin compared with control or chrysotile or tunicamycin-treated cells (Fig. 5*B*). This finding suggested that thapsigargin treatment caused some degree of ER Ca^{2+} depletion and thereby activated store-operated Ca^{2+} channels (29) within this time frame.

Because ER Ca^{2+} depletion induced ER stress, we next determined if ER stress modulated Ca^{2+} release in cells under ER stress. Cells were treated with chrysotile or thapsigargin or tunicamycin for 24 h and assayed for Ca^{2+} release using the Ca^{2+} ionophore, ionomycin. Ionomycin-releasable Ca^{2+} was greater in cells previously treated with chrysotile, thapsigargin, or tunicamycin compared with control cells (Fig. 5, *C* and *D*). Similar experiments were conducted to assess ER Ca^{2+} stores by asking if store-operated Ca^{2+} channels could be activated in cells under ER stress. As shown (Fig. 5, *E* and *F*), addition of 2 mM $CaCl_2$ to cells previously exposed to chrysotile, thapsigargin, or tunicamycin resulted in greater increases in cytosolic Ca^{2+} compared with control cells. Collectively, these findings suggest that macrophages under ER stress may exhibit increased ionomycin-releasable Ca^{2+} stores, yet these cells may still exhibit some degree of ER Ca^{2+} depletion.

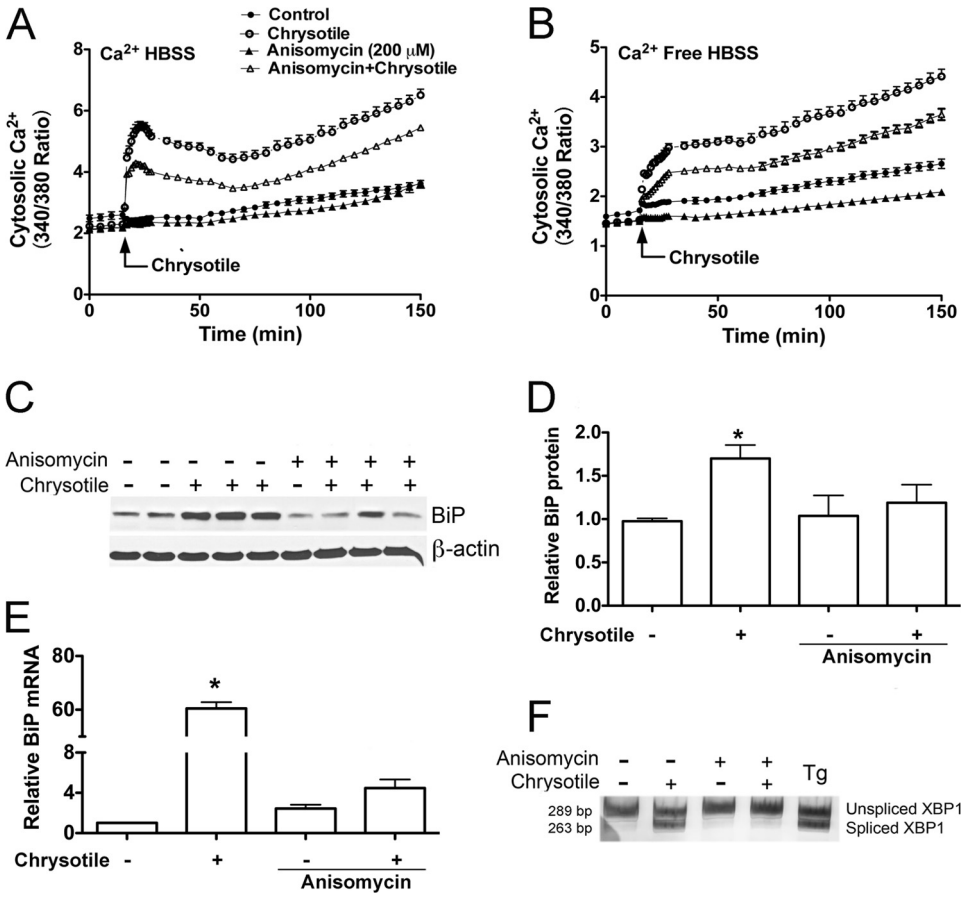

FIGURE 4. **Anisomycin treatment reduces cytosolic Ca^{2+} levels and modulates chrysotile-induced ER stress.** Cells were loaded with Fura2-AM (1 μM, 30 min, 37 °C) and suspended in either HBSS containing 1.3 mM Ca^{2+} HBSS (*A*) or Ca^{2+} free HBSS (*B*). Cells were incubated with 200 μM anisomycin for 60 min before exposure to chrysotile (10 $\mu g/cm^2$). Values are mean ± S.E. ($n = 6$/group). *C,* macrophages were pretreated with 0.2 μM anisomycin for 60 min before exposure to chrysotile (10 $\mu g/cm^2$) for 24 h. BiP protein in lysates was determined by immunoblot analysis. Data from experiments conducted as described in *C* are shown: *D,* densitometric analysis of BiP protein corrected for β-actin (mean ± S.E., 3 experiments); *E,* BiP mRNA corrected for hypoxanthine-guanine phosphoribosyltransferase mRNA assayed by quantitative RT-PCR (*, $p < 0.05$ *versus* control, mean ± S.E., 3 experiments); and *F*, XBP1 splicing was evaluated by conventional RT-PCR followed by acrylamide gel electrophoresis.

Because the IP_3R is an IP_3-gated channel that releases Ca^{2+} from the ER, and because modulation of IP_3R activity is considered important for life or death decisions made by cells under ER stress (30), we asked if knockdown of IP_3R-1, the major IP_3R isoform present in macrophages (31), would alter cytosolic Ca^{2+} levels in macrophages exposed to chrysotile. We found that cells transfected with IP_3R-1 siRNA showed significantly reduced IP_3R-1 mRNA levels (Fig. 5*G*); however, cytosolic Ca^{2+} levels were not altered by chrysotile exposure (Fig. 5*H*).

Expression of the UPR in Macrophages in Vivo and ex Vivo—Most prior studies have documented ER stress with activation of the UPR in AECs or in fibroblasts using various disease models (3, 32), whereas ER stress in alveolar macrophages from diseased lung has not been investigated. To evaluate ER stress in macrophages *in vivo*, C57BL/6 mice were exposed either to TiO_2 or chrysotile intratracheally and euthanized 21 days later. The lungs of mice exposed to TiO_2 were essentially normal. In contrast, chrysotile-exposed lungs showed destruction of normal lung architecture by widespread collagen deposition (Fig. 6*A*). The histological findings were confirmed biochemically by elevated hydroxyproline content in chrysotile-exposed lung tissue compared with TiO_2-exposed lungs (Fig. 6*B*). BAL samples from the two groups contained similar numbers of cells (~$8.9 \pm 4.4 \times 10^5$ cells/mouse), and the predominant cells were macrophages (Fig. 6*C*). The alveolar macrophages obtained from fibrotic mice showed elevated BiP protein compared with BAL cell lysates from TiO_2-exposed mice (Fig. 6, *D* and *E*). Quantitative RT-PCR from whole lung and BAL cells revealed elevated BiP transcript levels in BAL alveolar macrophages from chrysotile-exposed mice, but not in whole lung tissue in mice exposed to chrysotile (Fig. 6*F*). Because ER stress has been linked to increased apoptosis in AEC (8, 9, 11, 12) in fibrotic lung, we determined if ER stress was associated with increased apoptosis in mouse BAL cells. There was no difference in apoptosis in alveolar macrophages from chrysotile- or TiO_2-exposed mice, as measured by caspase-3 (Fig. 6, *G* and *H*). To link ER stress to the fibrotic response following chrysotile exposure, we measured active TGF-β1 in BAL fluid and found that it was elevated in fibrotic mice compared with the TiO_2-exposed mice (Fig. 6*I*). In aggregate, these data suggest that the UPR induces cell survival in macrophages and that macrophage survival is an important determinant of fibrosis development.

To support findings from fibrotic mice, BAL cells from normal subjects and asbestosis patients were evaluated for ER stress. Consistent with our *in vitro* and *in vivo* findings, BAL cell lysates from asbestosis patients showed increased levels of BiP

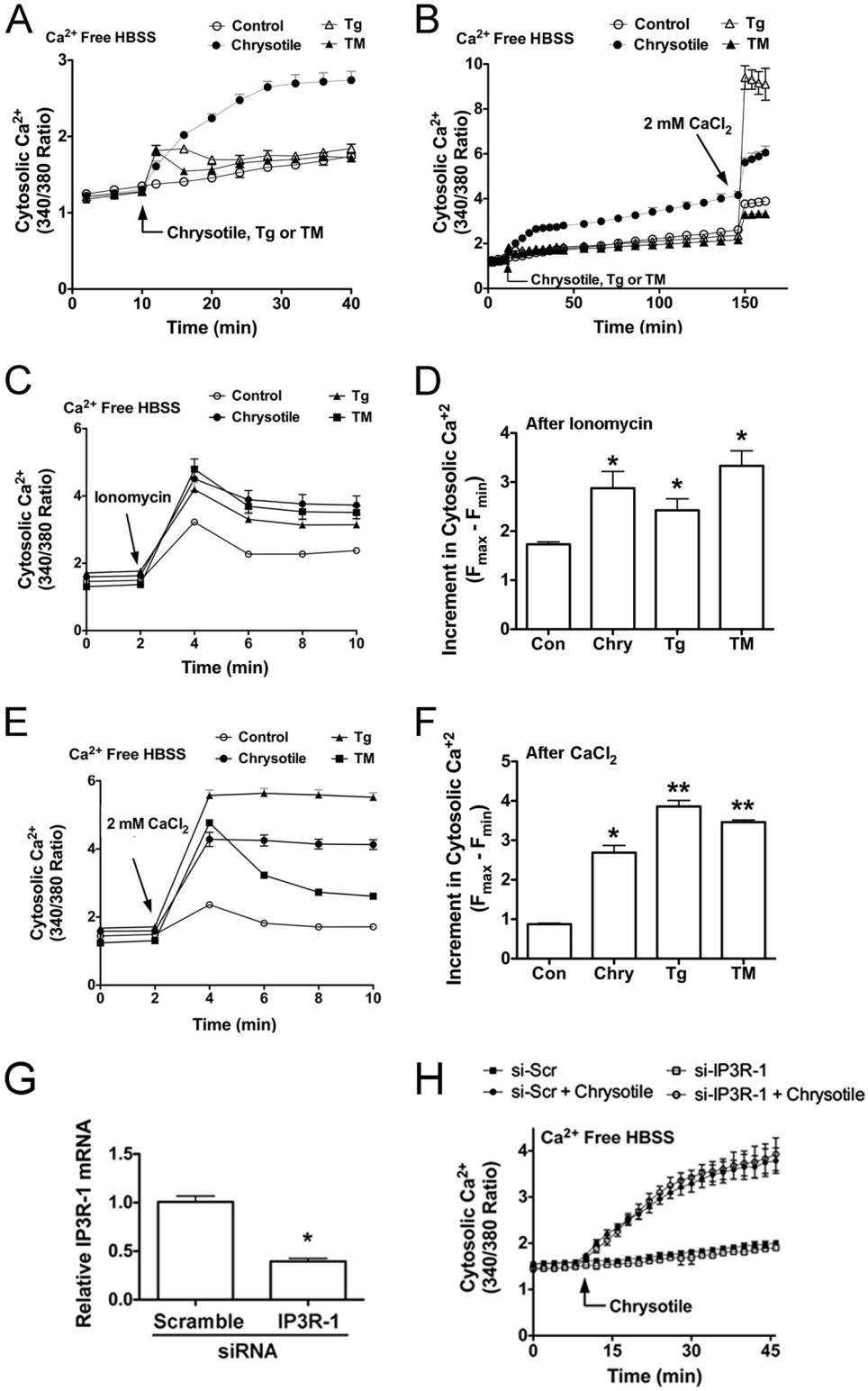

FIGURE 5. **Chrysotile increases ionomycin-releasable calcium stores and alters activation of store-operated Ca^{2+} channels in macrophages.** *A,* cells were loaded with Fura2-AM (1 μM, 30 min, 37 °C), suspended in Ca^{2+}-free HBSS, and exposed to chrysotile (10 μg/well), thapsigargin (*Tg*) (100 nM), or tunicamycin (*TM*) (5 μg/ml) followed by (*B*) 2 mM $CaCl_2$. Values are mean ± S.E. (n = 6/group). *C,* cells were exposed to chrysotile (10 μg/well), thapsigargin (100 nM), or tunicamycin (5 μg/ml) for 24 h and then assayed for Ca^{2+} release by ionomycin (5 μM). *D,* increments in cytosolic Ca^{2+} were determined by the maximum change in $F_{340/380}$ observed in the first 2 min after ionomycin. *, $p < 0.05$ *versus* control (n = 6/group). *E,* cells were exposed to chrysotile, thapsigargin, or tunicamycin for 24 h as described above, and then assayed for changes in cytosolic Ca^{2+} after addition of 2 mM $CaCl_2$. *F,* increments in cytosolic Ca^{2+} after $CaCl_2$ addition were determined as described in *D*. * or **, $p < 0.05$ *versus* control (n = 6/group). *E,* macrophages were transfected with either scrambled or IP3R-1 siRNA for 48 h and assayed for IP3R-1 mRNA by quantitative RT-PCR (*, $p < 0.05$ *versus* scramble) (*G*) and cytosolic Ca^{2+} levels after chrysotile exposure (*H*) (n = 6/group).

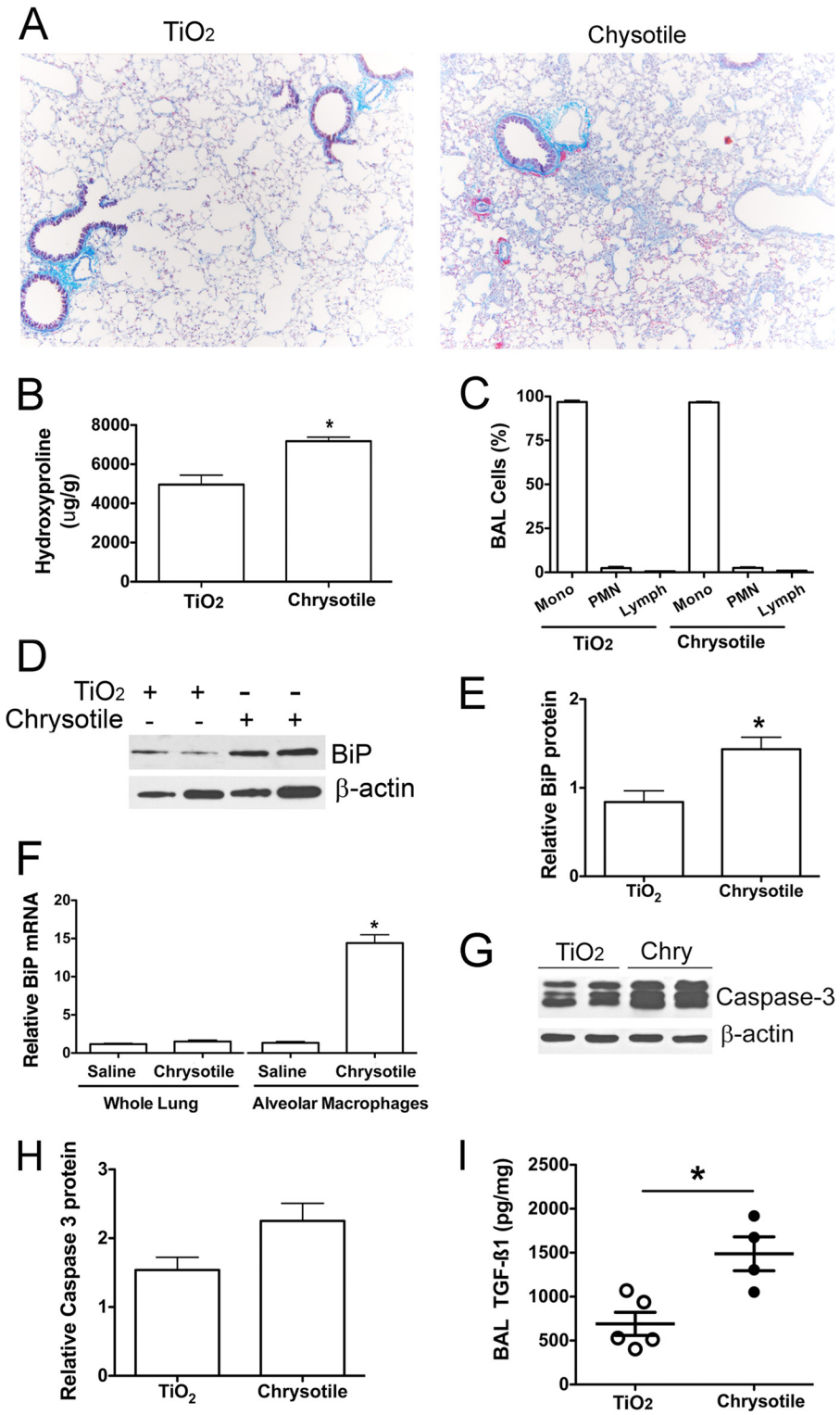

FIGURE 6. **ER stress is present in macrophages obtained from fibrotic lungs.** C57BL/6J mice were given either TiO_2 (125 μg) or chrysotile (125 μg) intratracheally. BAL and lung tissues were obtained 21 days after exposure. *A*, lung sections from mice exposed to TiO_2 or chrysotile were assayed by Masson's trichrome staining for detection of collagen deposition. *B*, hydroxyproline content of mouse lung exposed to TiO_2 or chrysotile for 21 days. *, $p < 0.05$ *versus* TiO_2 ($n = 6$/group). *C*, differential counts for BAL cells after Giemsa-Wright staining ($n = 6$/group). *D*, BAL cell lysates assayed by BiP protein immunoblotting. *E*, densitometric analysis of BiP protein expression corrected for β-actin; *, $p < 0.05$ *versus* TiO_2 ($n = 4$/group). *F*, total RNA from whole lung or from BAL cells was evaluated by quantitative RT-PCR for BiP mRNA normalized to β-actin mRNA. *, $p < 0.05$ *versus* other groups ($n = 3$/group). *G*, BAL cell lysates were assayed by protein immunoblotting for caspase-3 and β-actin. *H*, densitometric analysis of caspase-3 protein corrected for β-actin ($n = 4$/group, $p = 0.06$). *I*, BAL fluid assayed for TGF-β1 by ELISA. Values normalized to BAL protein, $n = 4$–5/group.

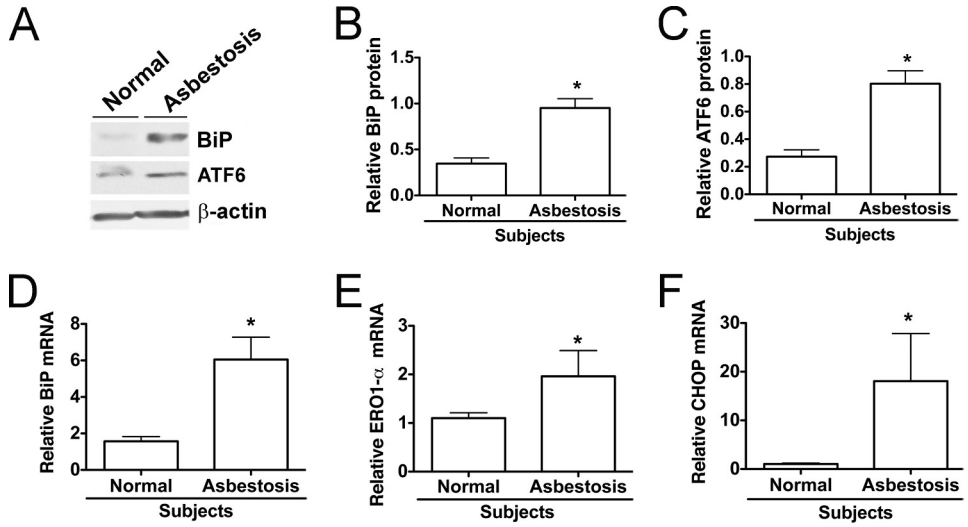

FIGURE 7. **Alveolar macrophages obtained from asbestosis patients show indicators of ER stress.** *A*, alveolar macrophage lysates used for assay of BiP and ATF6 protein expression by immunoblotting. *B* and *C*, densitometric analysis of BiP and ATF6 protein expression normalized to β-actin in normal subjects and asbestosis patients. *, $p < 0.05$ *versus* normal subjects ($n = 3–4$/group). *D–F*, quantitative RT-PCR data showing mRNA of different ER stress genes corrected for hypoxanthine-guanine phosphoribosyltransferase mRNA. *, $p < 0.05$ *versus* normal subjects ($n = 3$/group).

protein as well as elevated ATF6α (Fig. 7*A*). Densitometric analysis of immunoblots revealed a significant increase in BiP protein (Fig. 7*B*) as well as ATF6α (Fig. 7*C*) in alveolar macrophages from asbestosis patients compared with normal subjects. We also found that alveolar macrophages from asbestosis patients had an increase in BiP mRNA, endoplasmic oxidase 1-α (ERO1-α), and DNA-damage inducible protein (CHOP) mRNA levels compared with normal subjects (Fig. 7, *D–F*). In aggregate, these observations suggest that ER stress in alveolar macrophages is linked to the asbestos-induced pulmonary fibrosis and alleviation of ER stress may be a novel target for therapy.

DISCUSSION

ER stress and the UPR are key pathogenic events in disease processes as different as atherosclerosis, heart disease, diabetes, cancer, and pulmonary fibrosis (4–6, 33). Regarding fibrosis, most available evidence indicates that ER stress enhances the vulnerability of structural cells such as AECs and fibroblasts to fibrotic stimuli. In these studies, ER stress and UPR in AECs has been associated with herpesvirus infection (9, 11), altered surfactant protein processing (9), expression of mutant surfactant proteins (9, 10, 34, 35), apoptosis (8, 11, 12), epithelial-mesenchymal transitions (7), and induction of an inflammatory response (35) that ultimately leads to a profibrotic environment in lung tissue (2, 3). To our knowledge, no studies have examined the UPR in macrophages in the setting of lung fibrosis.

The objective of this study was to investigate ER stress in alveolar macrophages exposed to chrysotile and to link ER Ca^{2+} release to induction of ER stress. Similar to a prior study using A549 cells (12), chrysotile asbestos exposure triggered rapid and sustained increases in cytosolic Ca^{2+} within minutes and increased ER stress markers (IRE1/XBP1 mRNA splicing, GRP78/BiP, and ATF6α) within 24 h. Chrysotile-induced increases in cytosolic Ca^{2+} were partially inhibited by anisomycin, an inhibitor of passive Ca^{2+} leak from the ER (22), or BAPTA-AM, a Ca^{2+} chelator known to deplete ER Ca^{2+} stores (20). Anisomycin inhibited induction of ER stress markers, whereas BAPTA enhanced ER stress, results suggesting that ER calcium depletion may be one factor contributing to ER stress in macrophages exposed to chrysotile.

ER Ca^{2+} stores are essential for protein folding as well as Ca^{2+} signaling, and thus ER Ca^{2+} depletion may act as an important upstream event in the pathogenesis of many diseases (16). Under basal and stimulated conditions, ER Ca^{2+} stores are dependent on many cellular processes, including mitochondrial ATP production, store-operated Ca^{2+} influx, ER Ca^{2+}-ATPase activity, and ER Ca^{2+} leak. Presumably, impairments in any of these cellular processes can contribute to ER stress in macrophages exposed to chrysotile. Our findings indicate that external sources as well as the ER Ca^{2+} stores are important for Ca^{2+} release in cells exposed to chrysotile. Because we found that chrysotile elicits prolonged ER Ca^{2+} release, we hypothesized that ER Ca^{2+} depletion modulates ER stress in macrophages.

Recently, ER Ca^{2+} leak through the translocon, an ER protein complex involved in translation, has been shown to be a possible site for ER Ca^{2+} depletion leading to activation of the UPR (21, 22). Translocons are protein-conducting channels found on the surface of rough ER. When ribosome-translocon complexes are free of polypeptide chains they remain open and conduct both ions and neutral molecules (36). To evaluate Ca^{2+} leak through the translocon, we used anisomycin (an inhibitor of peptidyltransferase) to maintain the ribosome-bound translocon in a closed state that reduces permeability to Ca^{2+} (22). We found that anisomycin partially inhibited chrysotile-induced increases in cytosolic Ca^{2+} in macrophages incubated in 1.3 mM Ca^{2+} and Ca^{2+}-free media. These finding are consistent with studies that showed inhibition of the translocon reduced thapsigargin-induced ER Ca^{2+} release in cells incubated in Ca^{2+}-free media (21, 28) and support the idea that ER Ca^{2+} leak occurs in cells exposed to chrysotile.

ER Ca^{2+} leak may not be the only factor contributing to ER Ca^{2+} release and depletion in chrysotile-exposed macrophages. Oxidative stress can trigger ER stress and promote ER Ca^{2+} release (18), perhaps by inhibiting ER Ca^{2+}-ATPase activity (37). Alternatively, IP_3R is an IP_3-gated channel that releases Ca^{2+} from the ER and is activated by IP_3, Ca^{2+}, and oxidative stress (30). We found that knockdown of IP_3R-1 did not alter chrysotile-induced increases in cytosolic Ca^{2+}; however, our Ca^{2+} measurements were obtained from a population of cells, which may not provide the resolution necessary for detecting changes in Ca^{2+} within a single cell or within mitochondria (31, 38). IP_3R-1 has been shown to be important for transferring Ca^{2+} directly to the mitochondria (38). A recent study in macrophages provided evidence for an UPR-CHOP-ERO1-α pathway triggering IP_3R-1-mediated Ca^{2+} release and apoptosis (31). Although our data suggest the involvement of the translocon and ER Ca^{2+} depletion in mediating ER stress, these observations do not exclude the contribution(s) of other mechanisms, including a possible role for IP_3R-1.

The current study demonstrates that BiP expression was elevated in alveolar macrophages obtained from human asbestosis patients and from mice with a fibrotic phenotype. BiP is known as the master regulator of the UPR (6), and BiP protein up-regulation is often used as an indicator of ER stress (39). To date the only known mechanism for activation of IRE1, PKR-like ER kinase, or ATF6 is their release from BiP, although the mechanisms behind the differential activation of the different arms of the UPR are not fully understood (40). We found that chrysotile exposure increased expression of various chaperone genes (endoplasmic-resident protein 72, GRP94, and protein kinase inhibitor 58-kDa) as well as other ER stress markers including ERO1-α and CHOP. Prior studies have evaluated the role of ER stress in inducing apoptosis in AEC as a potential mechanism in the pathogenesis of pulmonary fibrosis (8, 9, 11, 12, 34). Our findings clearly reveal ER stress in chrysotile-exposed macrophages; however, we found no significant apoptosis in alveolar macrophages from chrysotile-exposed mice. As previously shown, these observations suggest that ER stress in macrophages exposed to chrysotile induces cell survival (38, 41, 42). Several chronic diseases have demonstrated that macrophage cell survival has an important role in disease progression (43–46). Our observations suggest that the UPR induce cell survival in macrophages, which mediates fibrosis development in lung. Moreover, the presence of ER stress in alveolar macrophages from fibrotic mice is significant in that lung homogenates did not exhibit elevated BiP expression suggesting that macrophages are an important mediator of the fibrotic response.

Stimulated macrophages display many different functions thought to be important for the pathogenesis of many disease states (47). Recent evidence indicates that alternatively activated (M2) macrophages are abundant in atherosclerotic lesions (48), and induction of ER stress induces macrophage polarization from the M1 into the M2 phenotype leading to increased cholesterol deposition and enhanced foam cell formation (49). Similar to the pro-inflammatory state induced by ER stress in AECs (35), ER stress in macrophages has been associated with pro-inflammatory effects through activation of both a JNK-TNFα pathway and a CHOP-ERK-IL-6 pathway (50). When exposed to chrysotile, macrophages produce pro-fibrotic cytokines such as TGF-β as well as high levels of reactive oxygen species, including H_2O_2 (13–15). In a recent study, we found that alveolar macrophages from asbestosis patients produce high levels of H_2O_2, and these cells demonstrate a predominantly pro-fibrotic M2 phenotype. Moreover, polarization to the M2 phenotype was driven, in part, by Cu,Zn-superoxide dismutase-mediated H_2O_2 production in chrysotile-exposed cells (13). Our new observations demonstrate that chrysotile-exposed macrophages exhibit rapid and sustained increases in Ca^{2+} release and later develop ER stress. More importantly, alveolar macrophages obtained from asbestosis patients or from mice with a fibrotic phenotype exhibit ER stress. Because the predominance of M2 macrophages are linked to the development of fibrosis, it will be interesting in future studies to alter ER stress *in vivo* and investigate polarization of macrophages and its relationship to fibrosis.

Acknowledgments—We thank Thomas Moninger and the University of Iowa Central Microscopy Research Facilities for assistance with the confocal microscope studies.

REFERENCES

1. Guidotti, T. L., Miller, A., Christiani, D., Wagner, G., Balmes, J., Harber, P., Brodkin, C. A., Rom, W., Hillerdal, G., Harbut, M., and Green, F. H. Y. (2004) Diagnosis and initial management of nonmalignant diseases related to asbestos. *Am. J. Respir. Crit. Care Med.* **170,** 691–715
2. Lenna, S., and Trojanowska, M. (2012) The role of endoplasmic reticulum stress and the unfolded protein response in fibrosis. *Curr. Opin. Rheumatol.* **24,** 663–668
3. Tanjore, H., Blackwell, T. S., and Lawson, W. E. (2012) Emerging evidence for endoplasmic reticulum stress in the pathogenesis of idiopathic pulmonary fibrosis. *Am. J. Physiol. Lung Cell. Mol. Physiol.* **302,** L721–729
4. Hetz, C. (2012) The unfolded protein response: controlling cell fate decisions under ER stress and beyond. *Nat. Rev. Mol. Cell Biol.* **13,** 89–102
5. Kim, I., Xu, W., and Reed, J. C. (2008) Cell death and endoplasmic reticulum stress: disease relevance and therapeutic opportunities. *Nat. Rev. Drug Discov.* **7,** 1013–1030
6. Xu, C., Bailly-Maitre, B., and Reed, J. C. (2005) Endoplasmic reticulum stress: cell life and death decisions. *J. Clin. Investig.* **115,** 2656–2664
7. Baek, H. A., Kim do, S., Park, H. S., Jang, K. Y., Kang, M. J., Lee, D. G., Moon, W. S., Chae, H. J., and Chung, M. J. (2012) Involvement of endoplasmic reticulum stress in myofibroblastic differentiation of lung fibroblasts. *Am. J. Respir. Cell Mol. Biol.* **46,** 731–739
8. Korfei, M., Ruppert, C., Mahavadi, P., Henneke, I., Markart, P., Koch, M., Lang, G., Fink, L., Bohle, R. M., Seeger, W., Weaver, T. E., and Guenther, A. (2008) Epithelial endoplasmic reticulum stress and apoptosis in sporadic idiopathic pulmonary fibrosis. *Am. J. Respir. Crit. Care Med.* **178,** 838–846
9. Lawson, W. E., Crossno, P. F., Polosukhin, V. V., Roldan, J., Cheng, D. S., Lane, K. B., Blackwell, T. R., Xu, C., Markin, C., Ware, L. B., Miller, G. G., Loyd, J. E., and Blackwell, T. S. (2008) Endoplasmic reticulum stress in alveolar epithelial cells is prominent in IPF: association with altered surfactant protein processing and herpesvirus infection. *Am. J. Physiol. Lung Cell. Mol. Physiol.* **294,** L1119–1126
10. Maitra, M., Wang, Y., Gerard, R. D., Mendelson, C. R., and Garcia, C. K. (2010) Surfactant protein A2 mutations associated with pulmonary fibrosis lead to protein instability and endoplasmic reticulum stress. *J. Biol. Chem.* **285,** 22103–22113
11. Torres-González, E., Bueno, M., Tanaka, A., Krug, L. T., Cheng, D. S.,

Polosukhin, V. V., Sorescu, D., Lawson, W. E., Blackwell, T. S., Rojas, M., and Mora, A. L. (2012) Role of endoplasmic reticulum stress in age-related susceptibility to lung fibrosis. *Am. J. Respir. Cell Mol. Biol.* **46,** 748–756

12. Kamp, D. W., Liu, G., Cheresh, P., Kim, S. J., Mueller, A., Lam, A. P., Trejo, H., Williams, D., Tulasiram, S., Baker, M., Ridge, K., Chandel, N. S., and Beri, R. (2013) Asbestos-induced alveolar epithelial cell apoptosis. The role of endoplasmic reticulum stress response. *Am. J. Respir. Cell Mol. Biol.* **49,** 892–901
13. He, C., Ryan, A. J., Murthy, S., and Carter, A. B. (2013) Accelerated development of pulmonary fibrosis via Cu,Zn-superoxide dismutase-induced alternative activation of macrophages. *J. Biol. Chem.* **288,** 20745–20757
14. Murthy, S., Adamcakova-Dodd, A., Perry, S. S., Tephly, L. A., Keller, R. M., Metwali, N., Meyerholz, D. K., Wang, Y., Glogauer, M., Thorne, P. S., and Carter, A. B. (2009) Modulation of reactive oxygen species by Rac1 or catalase prevents asbestos-induced pulmonary fibrosis. *Am. J. Physiol. Lung Cell Mol. Physiol.* **297,** 846–855
15. Osborn-Heaford, H. L., Ryan, A. J., Murthy, S., Racila, A. M., He, C., Sieren, J. C., Spitz, D. R., and Carter, A. B. (2012) Mitochondrial Rac1 GTPase import and electron transfer from cytochrome *c* are required for pulmonary fibrosis. *J. Biol. Chem.* **287,** 3301–3312
16. Mekahli, D., Bultynck, G., Parys, J. B., De Smedt, H., and Missiaen, L. (2011) Endoplasmic-reticulum calcium depletion and disease. *Cold Spring Harb. Perspect. Biol.* **3,** a004317
17. Thastrup, O., Cullen, P. J., Drøbak, B. K., Hanley, M. R., and Dawson, A. P. (1990) Thapsigargin, a tumor promoter, discharges intracellular Ca^{2+} stores by specific inhibition of the endoplasmic reticulum Ca^{2+}-ATPase. *Proc. Natl. Acad. Sci. U. S. A.* **87,** 2466–2470
18. Dejeans, N., Tajeddine, N., Beck, R., Verrax, J., Taper, H., Gailly, P., and Calderon, P. B. (2010) Endoplasmic reticulum calcium release potentiates the ER stress and cell death caused by an oxidative stress in MCF-7 cells. *Biochem. Pharmacol.* **79,** 1221–1230
19. Nakano, T., Watanabe, H., Ozeki, M., Asai, M., Katoh, H., Satoh, H., and Hayashi, H. (2006) Endoplasmic reticulum Ca^{2+} depletion induces endothelial cell apoptosis independently of caspase-12. *Cardiovasc. Res.* **69,** 908–915
20. Yoshida, I., Monji, A., Tashiro, K., Nakamura, K., Inoue, R., and Kanba, S. (2006) Depletion of intracellular Ca^{2+} store itself may be a major factor in thapsigargin-induced ER stress and apoptosis in PC12 cells. *Neurochem. Int.* **48,** 696–702
21. Flourakis, M., Van Coppenolle, F., Lehen'kyi, V., Beck, B., Skryma, R., and Prevarskaya, N. (2006) Passive calcium leak via translocon is a first step for iPLA2-pathway regulated store operated channels activation. *FASEB J.* **20,** 1215–1217
22. Van Coppenolle, F., Vanden Abeele, F., Slomianny, C., Flourakis, M., Hesketh, J., Dewailly, E., and Prevarskaya, N. (2004) Ribosome-translocon complex mediates calcium leakage from endoplasmic reticulum stores. *J. Cell Sci.* **117,** 4135–4142
23. Weischenfeldt, J., and Porse, B. (2008) Bone marrow-derived macrophages (BMM): isolation and applications. *CSH Protoc.* 10.1101/pdb.prot5080
24. Carter, A. B., Knudtson, K. L., Monick, M. M., and Hunninghake, G. W. (1999) The p38 mitogen-activated protein kinase is required for NF-κB-dependent gene expression: the role of TATA-binding protein (TBP). *J. Biol. Chem.* **274,** 30858–30863
25. Samali, A., Fitzgerald, U., Deegan, S., and Gupta, S. (2010) Methods for monitoring endoplasmic reticulum stress and the unfolded protein response. *Int. J. Cell Biol.* **2010,** 830307
26. Adachi, Y., Yamamoto, K., Okada, T., Yoshida, H., Harada, A., and Mori, K. (2008) ATF6 is a transcription factor specializing in the regulation of quality control proteins in the endoplasmic reticulum. *Cell Struct. Funct.* **33,** 75–89
27. Wu, J., Rutkowski, D. T., Dubois, M., Swathirajan, J., Saunders, T., Wang, J., Song, B., Yau, G. D., and Kaufman, R. J. (2007) ATF6α optimizes long-term endoplasmic reticulum function to protect cells from chronic stress. *Developmental cell* **13,** 351–364
28. Hammadi, M., Oulidi, A., Gackière, F., Katsogiannou, M., Slomianny, C., Roudbaraki, M., Dewailly, E., Delcourt, P., Lepage, G., Lotteau, S., Ducreux, S., Prevarskaya, N., and Van Coppenolle, F. (2013) Modulation of ER stress and apoptosis by endoplasmic reticulum calcium leak via translocon during unfolded protein response: involvement of GRP78. *FASEB J.* **27,** 1600–1609
29. Ma, H. T., Patterson, R. L., van Rossum, D. B., Birnbaumer, L., Mikoshiba, K., and Gill, D. L. (2000) Requirement of the inositol trisphosphate receptor for activation of store-operated Ca^{2+} channels. *Science* **287,** 1647–1651
30. Kiviluoto, S., Vervliet, T., Ivanova, H., Decuypere, J. P., De Smedt, H., Missiaen, L., Bultynck, G., and Parys, J. B. (2013) Regulation of inositol 1,4,5-trisphosphate receptors during endoplasmic reticulum stress. *Biochim. Biophys. Acta* **1833,** 1612–1624
31. Li, G., Mongillo, M., Chin, K. T., Harding, H., Ron, D., Marks, A. R., and Tabas, I. (2009) Role of ERO1-α-mediated stimulation of inositol 1,4,5-triphosphate receptor activity in endoplasmic reticulum stress-induced apoptosis. *J. Cell Biol.* **186,** 783–792
32. Liu, G., Beri, R., Mueller, A., and Kamp, D. W. (2010) Molecular mechanisms of asbestos-induced lung epithelial cell apoptosis. *Chem-Biol. Interact.* **188,** 309–318
33. Wynn, T. A. (2011) Integrating mechanisms of pulmonary fibrosis. *J. Exp. Med.* **208,** 1339–1350
34. Lawson, W. E., Cheng, D. S., Degryse, A. L., Tanjore, H., Polosukhin, V. V., Xu, X. C., Newcomb, D. C., Jones, B. R., Roldan, J., Lane, K. B., Morrisey, E. E., Beers, M. F., Yull, F. E., and Blackwell, T. S. (2011) Endoplasmic reticulum stress enhances fibrotic remodeling in the lungs. *Proc. Natl. Acad. Sci. U. S. A.* **108,** 10562–10567
35. Maguire, J. A., Mulugeta, S., and Beers, M. F. (2011) Endoplasmic reticulum stress induced by surfactant protein C BRICHOS mutants promotes proinflammatory signaling by epithelial cells. *Am. J. Respir. Cell Mol. Biol.* **44,** 404–414
36. Hamman, B. D., Hendershot, L. M., and Johnson, A. E. (1998) BiP maintains the permeability barrier of the ER membrane by sealing the lumenal end of the translocon pore before and early in translocation. *Cell* **92,** 747–758
37. Kaplan, P., Babusikova, E., Lehotsky, J., and Dobrota, D. (2003) Free radical-induced protein modification and inhibition of Ca^{2+}-ATPase of cardiac sarcoplasmic reticulum. *Mol. Cell. Biochem.* **248,** 41–47
38. Hayashi, T., and Su, T. P. (2007) Sigma-1 receptor chaperones at the ER-mitochondrion interface regulate Ca^{2+} signaling and cell survival. *Cell* **131,** 596–610
39. Cawley, K., Deegan, S., Samali, A., and Gupta, S. (2011) Assays for detecting the unfolded protein response. *Methods Enzymol.* **490,** 31–51
40. Ron, D., and Walter, P. (2007) Signal integration in the endoplasmic reticulum unfolded protein response. *Nat. Rev. Mol. Cell Biol.* **8,** 519–529
41. Ogata, M., Hino, S., Saito, A., Morikawa, K., Kondo, S., Kanemoto, S., Murakami, T., Taniguchi, M., Tanii, I., Yoshinaga, K., Shiosaka, S., Hammarback, J. A., Urano, F., and Imaizumi, K. (2006) Autophagy is activated for cell survival after endoplasmic reticulum stress. *Mol. Cell. Biol.* **26,** 9220–9231
42. Cullinan, S. B., and Diehl, J. A. (2004) PERK-dependent activation of Nrf2 contributes to redox homeostasis and cell survival following endoplasmic reticulum stress. *J. Biol. Chem.* **279,** 20108–20117
43. Duffield, J. S., Forbes, S. J., Constandinou, C. M., Clay, S., Partolina, M., Vuthoori, S., Wu, S., Lang, R., and Iredale, J. P. (2005) Selective depletion of macrophages reveals distinct, opposing roles during liver injury and repair. *J. Clin. Investig.* **115,** 56–65
44. Pechkovsky, D. V., Prasse, A., Kollert, F., Engel, K. M., Dentler, J., Luttmann, W., Friedrich, K., Müller-Quernheim, J., and Zissel, G. (2010) Alternatively activated alveolar macrophages in pulmonary fibrosis-mediator production and intracellular signal transduction. *Clin. Immunol.* **137,** 89–101
45. Shechter, R., Miller, O., Yovel, G., Rosenzweig, N., London, A., Ruckh, J., Kim, K. W., Klein, E., Kalchenko, V., Bendel, P., Lira, S. A., Jung, S., and Schwartz, M. (2013) Recruitment of beneficial M2 macrophages to injured spinal cord is orchestrated by remote brain choroid plexus. *Immunity* **38,** 555–569
46. Weigert, A., Johann, A. M., von Knethen, A., Schmidt, H., Geisslinger, G., and Brüne, B. (2006) Apoptotic cells promote macrophage survival by releasing the antiapoptotic mediator sphingosine-1-phosphate. *Blood*

108, 1635–1642
47. Wynn, T. A., and Barron, L. (2010) Macrophages: master regulators of inflammation and fibrosis. *Semin. Liver Dis.* **30,** 245–257
48. Bouhlel, M. A., Derudas, B., Rigamonti, E., Dièvart, R., Brozek, J., Haulon, S., Zawadzki, C., Jude, B., Torpier, G., Marx, N., Staels, B., and Chinetti-Gbaguidi, G. (2007) PPARγ activation primes human monocytes into alternative M2 macrophages with anti-inflammatory properties. *Cell Metab.* **6,** 137–143
49. Oh, J., Riek, A. E., Weng, S., Petty, M., Kim, D., Colonna, M., Cella, M., and Bernal-Mizrachi, C. (2012) Endoplasmic reticulum stress controls M2 macrophage differentiation and foam cell formation. *J. Biol. Chem.* **287,** 11629–11641
50. Li, Y., Schwabe, R. F., DeVries-Seimon, T., Yao, P. M., Gerbod-Giannone, M. C., Tall, A. R., Davis, R. J., Flavell, R., Brenner, D. A., and Tabas, I. (2005) Free cholesterol-loaded macrophages are an abundant source of tumor necrosis factor-α and interleukin-6: model of NF-κB- and map kinase-dependent inflammation in advanced atherosclerosis. *J. Biol. Chem.* **280,** 21763–21772